

SUPPLEMENTAL FIGURES

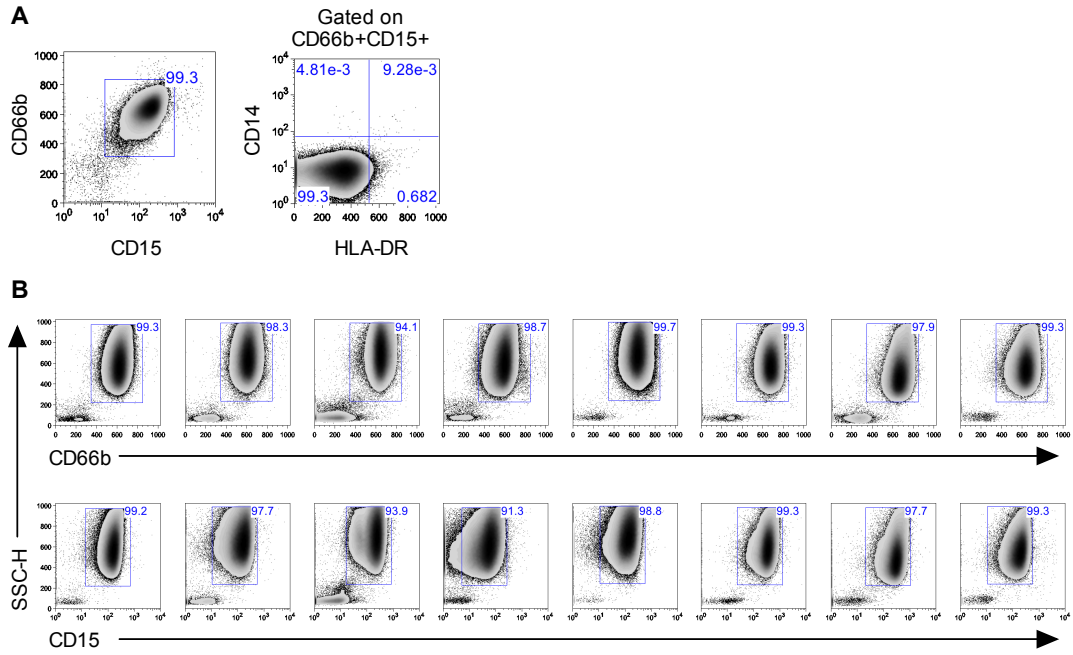


Figure S1. Characterization of neutrophils from *P. vivax*-infected patients. Related to Figure 1. Density plots of purified neutrophils from malaria patients confirming that these cells are positive for CD66b and CD15 (A and B). Neutrophils were also stained with monoclonal antibodies CD14 and HLA-DR to exclude monocyte contamination (A). Numbers beside each box refer to the cell frequencies within each gate.

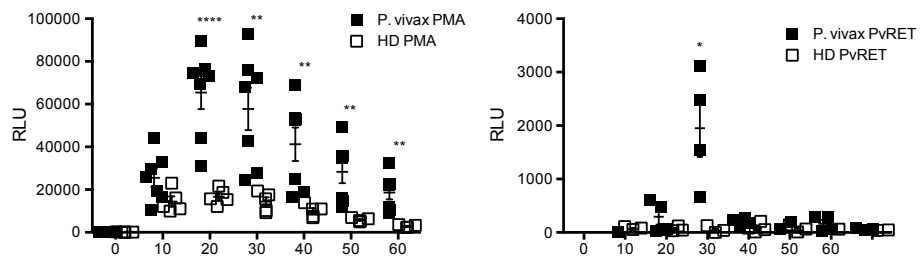


Figure S2. Neutrophils from *P. vivax*-infected patients display an enhanced ROS production. Related to Figure 1. Individual values of neutrophils ROS induction from *P. vivax*-infected patients (n=7) and healthy donors (n=5) stimulated with 100 ng/mL of PMA. Data of PvRET (PvRET:neutrophils ratio, 2:1) were obtained from four malaria patients and four healthy donors. The differences are relative to HDs neutrophils. *0.05<P<0.01; **0.01>P>0.001; ****P<0.0001.

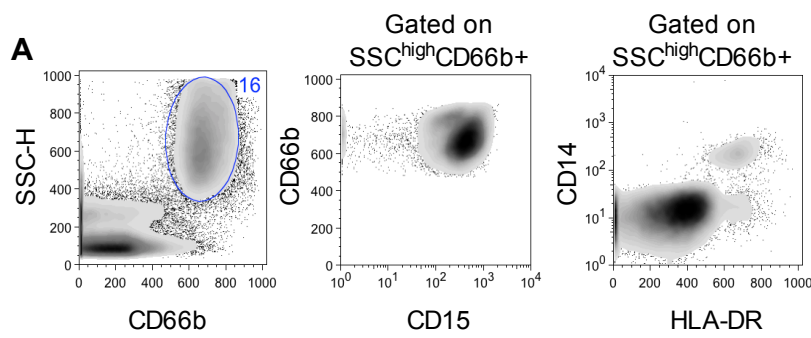


Figure S3. Characterization of LDGs from *P. vivax*-infected patients. Related to Figure 2. Representative density plots of LDGs from *P. vivax*-infected patients stained with different antibodies to better characterize the LDG subpopulation. First, $\text{SSC}^{\text{hi}}\text{CD66b}^+$ cells were selected within PBMCs. Then, we confirmed the expression of CD15 and the exclusion of CD14 and MHC-class II indicating that they were LDGs within PBMCs from patients with acute *P. vivax* infection.

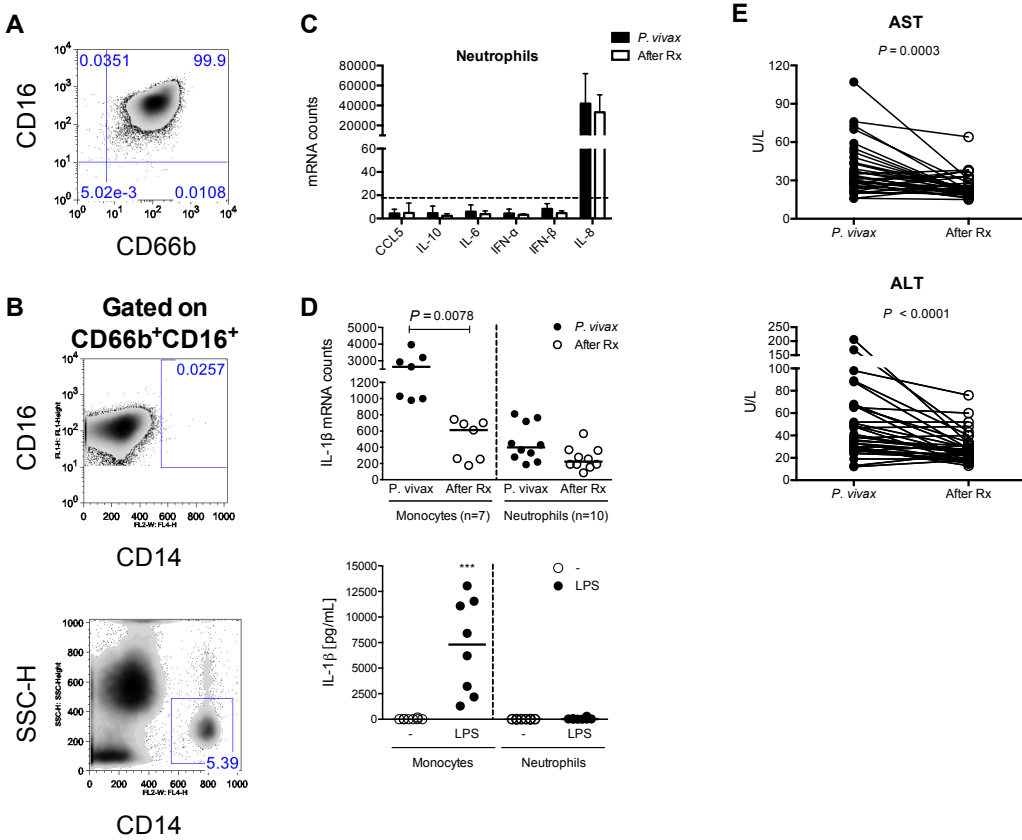


Figure S4. Validation and confirmation of neutrophils purity from *P. vivax*-infected patients. Related to Figure 4. (A) Representative density plot of highly purified CD66b⁺CD16⁺ cells used for nanostring assay. (B) Top panel: representative density plot of CD14⁺CD16⁺ cells gated on neutrophils. Bottom panel: CD14⁺ cells from PBMCs. (C) Nanostring mRNA counts of chemokines and cytokines of neutrophils from *P. vivax*-infected patients and the same individuals 30–45 days after treatment (After Rx). Dotted line is the limit of detection of the assay. IL-8 was used as a positive control. Data are presented as mean \pm SD (n=10). (D) Top panel: Highly purified neutrophils (n=10) and monocytes (n=7) from *P. vivax*-infected patients and the same individuals after chemotherapy were lysate and their mRNA expression was analyzed by nanostring. Paired T test or Wilcoxon signed rank when a normality test failed was performed and the P values are depicted in the graph. Bottom panel: Purified monocytes (n=8) or neutrophils (n=8) from *P. vivax*-infected subjects before and 30–45 days after treatment were cultured for 48 hours in the absence or presence of LPS (100 ng/mL). Protein levels of IL-1 β were measured in the supernatants of monocytes and neutrophils cultures. Significant differences are relative to the non-stimulated samples using unpaired t test. ***P<0.001. (E) Serum AST and ALT levels were measured in *P. vivax*-infected patients and the same individuals 30–45 days after chemotherapy. Each pair of circles connected by a line represents one patient before and after treatment (n=32).

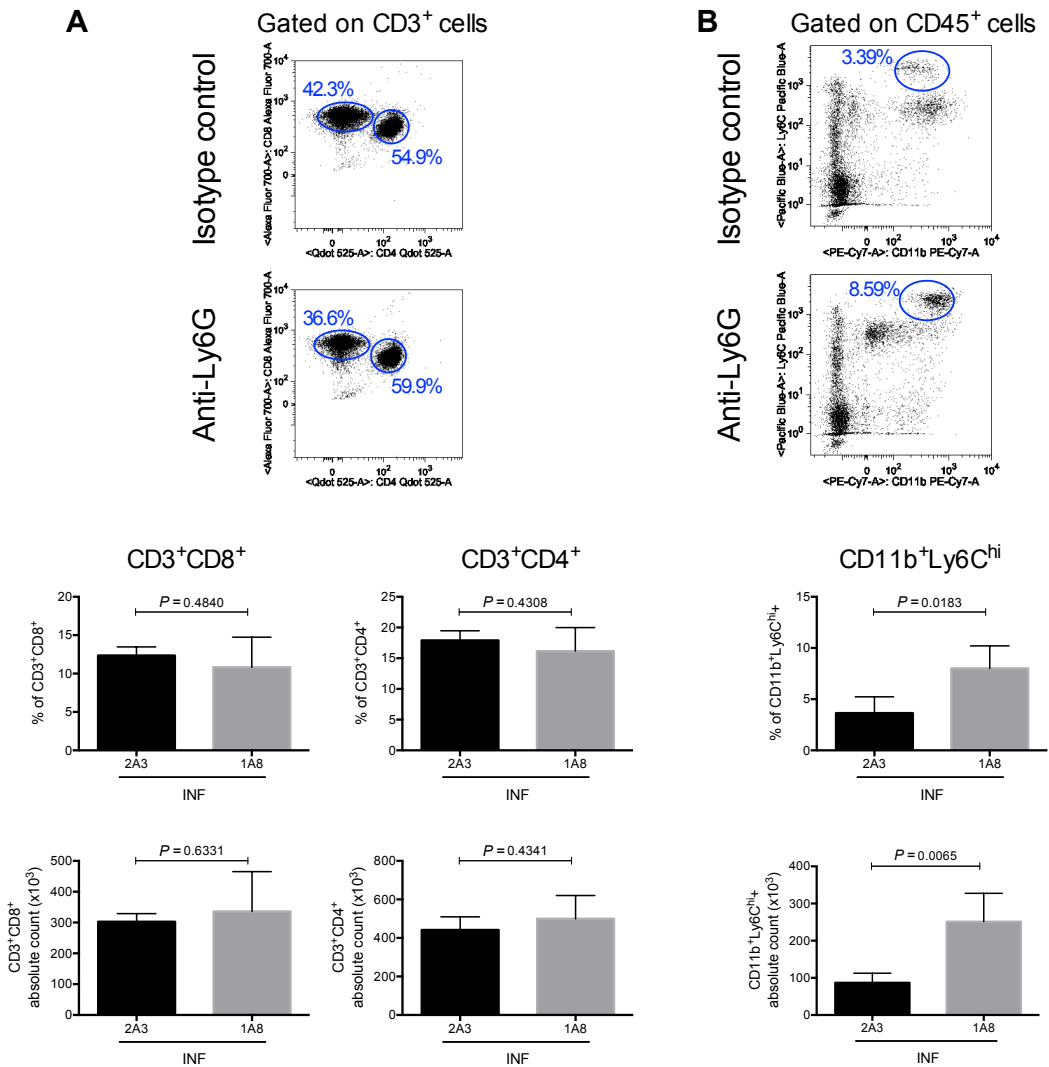


Figure S5. Neutrophil depletion affects liver leukocyte numbers after *P. chabaudi* infection. Related to Figure 5. Anti-Ly6G- (1A8) and isotype control-treated (2A3) animals were infected with *P. chabaudi*. After 11 days of infection, whole blood was harvested and different cell populations were analyzed by flow cytometry. (A) Top panels: Representative dot plots of CD8 $^+$ and CD4 $^+$ cells gated on CD3 $^+$ cells in infected mice followed by both treatments. Bottom panels: bar graph showing quantification of frequency and absolute numbers of CD3 $^+$ CD8 $^+$ cells (left panel) and CD3 $^+$ CD4 $^+$ cells (right panel). (B) Top panels: Representative dot plots of CD11b $^+$ Ly6C $^{\text{hi}}$ cells gated on CD45 $^+$ leukocytes in infected mice followed by both treatments. Bottom panels: bar graph showing quantification of frequency and absolute numbers of CD11b $^+$ Ly6C $^{\text{hi}}$ cells. Numbers within or beside each box refer to the cell frequencies within each gate. Data are represented as mean \pm SD (n=4).

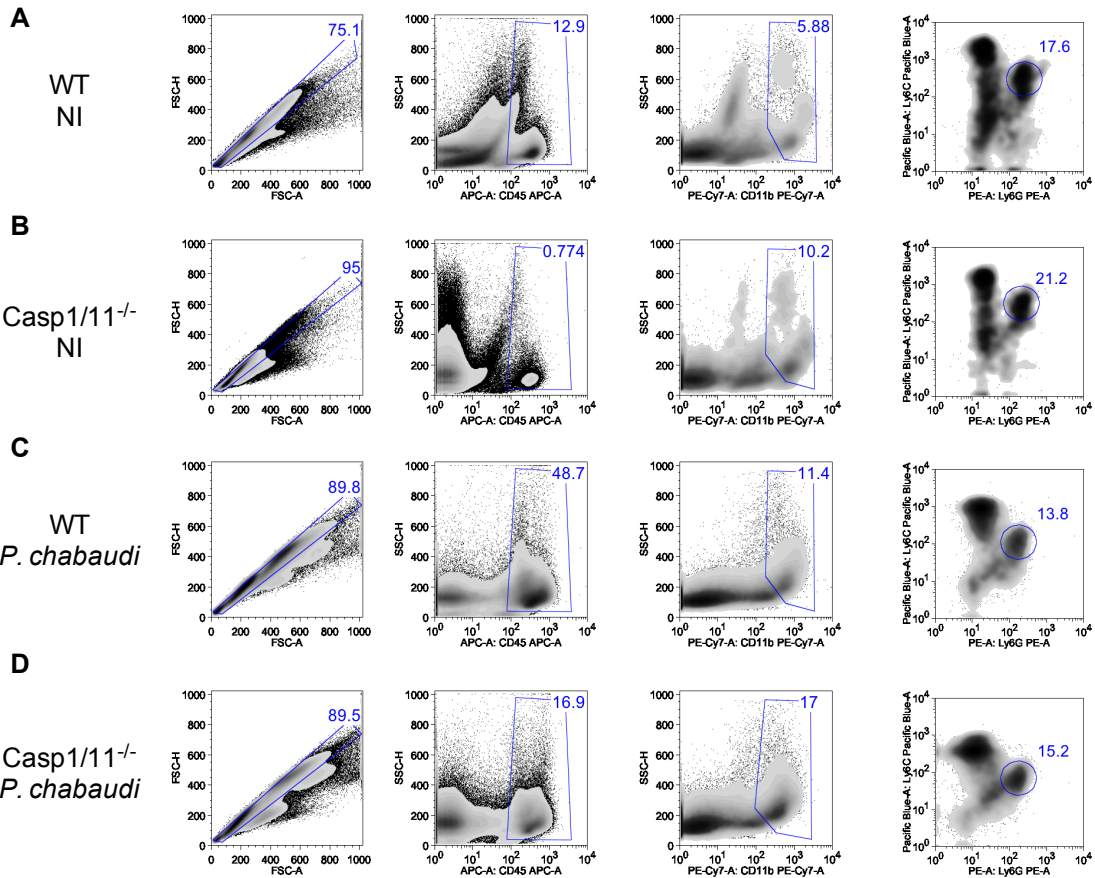


Figure S6. Caspase-1/11^{-/-} is associated with neutrophil recruitment to liver after *P. chabaudi* infection. Related to Figure 6. Gating strategy used to determine the frequencies of CD11b⁺Ly6C^{int}Ly6G⁺ cells in non-infected (A) WT and (B) Casp1/11^{-/-} mice, and in *P. chabaudi*-infected (C) WT and (D) Casp1/11^{-/-} mice. First, cells were gated on singlets, followed by CD45⁺, CD11b⁺ and later by Ly6G⁺Ly6C^{int}. Numbers within or beside each box refer to the cell frequencies within each gate.

Supplemental Tables

Table S1. List of genes expressed in neutrophils. Related to Figure 4. mRNA transcripts of neutrophils from *P. vivax*-infected before and after treatment (After Rx) patients by nanostring array. Transcripts were considered significant if FDR P value ≤ 0.05 and absolute fold change ≥ 1.8 . Accession ID is the GenBank accession number for each gene.

Gene name	Accession ID	Mean <i>P. vivax</i> mRNA counts	Mean After Rx mRNA counts	Fold change	P value
<i>CXCL10</i>	NM_001565.1	66.2719	2.6388	25.11	0.0328012
<i>VIPERIN</i>	NM_080657.4	1203.55	57.6876	20.86	0.0012727
<i>PSTPIP2</i>	NM_024430.3	1785.86	103.603	17.24	6.2193E-09
<i>SOCS1</i>	NM_003745.1	498.053	29.2685	17.02	0.00301039
<i>SAMHD1</i>	NM_015474.2	1916.53	161.195	11.89	2.26082E-07
<i>AIM2</i>	NM_004833.1	344.669	47.9981	7.18	0.000492025
<i>LGP2/DHX58</i>	NM_024119.2	91.2594	13.6714	6.68	0.00101801
<i>IRF7</i>	NM_001572.3	1845.45	303.99	6.07	0.00030156
<i>TAPI</i>	NM_000593.5	997.396	177.358	5.62	3.42627E-09
<i>IFIT2</i>	NM_001547.4	1650.51	327.407	5.04	0.00231986
<i>RIG-I</i>	NM_014314.3	1031.75	207.647	4.97	1.68086E-06
<i>A20</i>	NM_006290.2	2541.21	547.716	4.64	0.00233114
<i>NLRC5</i>	NM_032206.3	957.043	240.43	3.98	1.21649E-07
<i>IRF5</i>	NM_001098627.1	34.242	9.57543	3.58	0.00109198
<i>IFI16</i>	NM_005531.1	1896.99	545.064	3.48	6.44466E-06
<i>TAP2</i>	NM_000544.3	394.143	113.812	3.46	0.000217091
<i>CD40</i>	NM_001250.4	21.5228	6.24968	3.44	0.01391
<i>IFIT1</i>	NM_001548.3	781.577	239.358	3.27	0.00580819
<i>DHX36</i>	NM_020865.2	115.268	36.259	3.18	0.000267304
<i>IRAK3</i>	NM_007199.1	522.556	168.488	3.10	0.000575498
<i>ICAM1</i>	NM_000201.1	1472.12	521.786	2.82	6.85817E-05
<i>IFI30</i>	NM_006332.3	1321.52	469.168	2.82	4.30139E-05
<i>IL1RA</i>	NM_173842.1	2003.65	742.008	2.70	0.00350258
<i>BLIMPI</i>	NM_182907.1	214.848	80.8441	2.66	9.54879E-06
<i>NFKBIA</i>	NM_020529.1	7847.66	3008.01	2.61	0.0747339
<i>CASP1</i>	NM_033292.2	602.56	234.918	2.56	4.73556E-06
<i>NOS2</i>	NM_000625.4	87.8145	35.9261	2.44	1.69554E-05
<i>TLR5</i>	NM_003268.3	142.203	62.8468	2.26	0.00366582
<i>COX2</i>	NM_000963.1	6563.15	3296	1.99	0.0327201
<i>CASP4</i>	NM_001225.3	1392.28	703.272	1.98	4.23748E-06
<i>LY96</i>	NM_015364.2	1079.47	562.431	1.92	0.000644376
<i>IRF2</i>	NM_002199.2	419.694	232.129	1.81	1.09902E-05
<i>IL1B</i>	NM_000576.2	455.666	264.465	1.72	0.0370508
<i>TREXI</i>	NM_016381.3	146.295	85.4153	1.71	0.073186
<i>CCL4</i>	NM_002984.2	368.729	219.064	1.68	0.397213

<i>NLRC4</i>	NM_021209.3	48.233	28.8752	1.67	0.034274
<i>TLR4</i>	NM_138554.2	1525.26	942.858	1.62	3.21272E-05
<i>CCL3</i>	NM_002983.2	120.535	77.0199	1.56	0.354664
<i>TLR8</i>	NM_138636.3	728.658	470.2	1.55	0.0030198
<i>TLR2</i>	NM_003264.3	895.563	578.826	1.55	0.00362496
<i>REL</i>	NM_002908.2	132.019	85.8607	1.54	0.0167265
<i>NFKB2</i>	NM_002502.2	773.083	505.877	1.53	0.0693814
<i>NFKB1</i>	NM_003998.2	149.308	100.114	1.49	0.00051066
<i>IL8</i>	NM_000584.2	45518.4	30582.4	1.49	0.202457
<i>CRI</i>	NM_000651.4	1427.29	997.663	1.43	0.0790429
<i>SOCS3</i>	NM_003955.3	782.835	549.301	1.43	0.117382
<i>TGFB</i>	NM_000660.3	1250.28	884.959	1.41	0.00334888
<i>TNFA</i>	NM_000594.2	70.6174	52.6528	1.34	0.274758
<i>CD55</i>	NM_000574.3	64.8217	48.8454	1.33	0.237756
<i>IFNARI</i>	NM_000629.2	118.056	91.9391	1.28	0.104384
<i>TNFR1/TNFRSF1A</i>	NM_001065.2	1299.63	1067.65	1.22	0.035276
<i>DDX21</i>	NM_004728.2	221.44	187.112	1.18	0.378863
<i>TLR1</i>	NM_003263.3	1365.42	1165.85	1.17	0.109183
<i>MYD88</i>	NM_001172567.1	802.69	714.064	1.12	0.0923793
<i>IFNGR2</i>	NM_005534.3	1190.2	1060.96	1.12	0.141988
<i>CCR1</i>	NM_001295.2	479.183	437.615	1.09	0.711269
<i>HCK</i>	NM_002110.2	3084.81	2934.68	1.05	0.64654
<i>DHX9</i>	NM_001357.3	70.118	78.4462	0.89	0.51943
<i>NLRP12</i>	NM_033297.1	268.225	347.435	0.77	0.0287854
<i>CXCL2</i>	NM_002089.3	20.3762	27.2604	0.75	0.54469
<i>TLR6</i>	NM_006068.2	270.983	370.535	0.73	0.0231024
<i>PSTPIP1</i>	NM_003978.3	204.61	290.331	0.70	0.0123635
<i>NLRP3</i>	NM_004895.4	34.7495	59.3385	0.59	0.10656
<i>TLR9</i>	NM_017442.2	9.21098	23.1462	0.40	0.000538844
<i>NLRP6</i>	NM_138329.1	61.494	205.58	0.30	9.73443E-06
<i>HMOXI</i>	NM_002133.1	16.914	56.8915	0.30	0.00386765

Table S2. Study population. Related to Experimental Procedures. Demographic, clinical and hematological records of *P. vivax*-infected patients before and after treatment.

ID	Gender	Age	Nº of malaria	Parasites /µL	Symptoms				Hematological and Biochemical Records											
					Fever °C	Rigors	Hemoglobin g%		RBCs million/mm ³		Leukocytes /mm ³		Platelets mil/mm ³		AST U/L		ALT U/L		Total Bilirubin mg/dL	
							<i>P. vivax</i>	AT ^b	<i>P. vivax</i>	AT	<i>P. vivax</i>	AT	<i>P. vivax</i>	AT	<i>P. vivax</i>	AT	<i>P. vivax</i>	AT	<i>P. vivax</i>	AT
1	M	51	> 30	501-10000	- ^a	Yes	12.9	13.1	4.44	4.52	5500	8700	113	193	43	22	51	29	1.7	0.38
2	F	34	0	501-10000	39.2	Yes	10.7	11.6	3.69	3.77	3400	4600	42	191	48	22	169	43	1.37	0.6
3	M	62	10	501-10000	-	Yes	10.4	14.1	3.61	4.68	5000	7100	51	159	59	20	206	33	2.7	0.71
4	M	36	2	301-500	38.5	Yes	13.4	14.5	4.44	4.77	6000	6000	66	189	39	25	66	34	1.18	0.56
5	M	33	3	501-10000	39.8	Yes	13.8	13.3	5.27	5.05	5200	5200	86	170	76	64	98	76	0.6	0.55
6	M	40	> 10	501-10000	37.2	Yes	14.7	13.8	4.85	4.5	5800	5000	131	125	28	37	47	48	1.32	0.63
7	M	46	5	501-10000	-	No	13.8	13.1	4.88	4.54	6100	4300	202	179	23	33	26	31	0.9	0.6
8	M	60	>15	301-500	-	No	15.9	14	5.45	4.9	6600	7600	180	278	25	17	33	25	0.74	0.6
9	M	22	1	501-10000	-	Yes	13.9	-	5.14	-	7000	-	124	-	18	-	30	-	1.42	-
10	F	28	2	301-500	37.2	Yes	13.5	12	4.32	4	6600	6500	171	229	37	22	88	28	2.51	0.76
11	M	30	5	501-10000	39	Yes	15.1	12	5.36	4.4	8200	8000	93	224	26	20	29	13	1.56	0.6
12	F	26	1	301-500	39.7	Yes	11	13	3.8	4.4	2900	6500	98	262	28	16	27	22	1.03	0.6
13	M	22	3	501-10000	38.4	Yes	15	15.6	5.2	4.68	10000	5800	152	196	33	20	49	23	4.67	0.8
14	F	30	0	200-300	37.1	Yes	12.3	13.2	4.44	4.5	4900	5300	120	174	20	20	24	24	1.5	0.66
15	M	25	1	501-10000	37.2	No	14	15	5.13	5.4	6500	4900	94	158	35	38	52	52	2.45	0.56
16	M	20	3	> 10000	35.6	No	15	14.1	5.41	4.88	7400	4700	146	272	21	19	30	28	0.96	0.5
17	M	52	-	> 10000	35.5	Yes	8.1	-	2.82	-	9500	-	57	-	30	-	35	-	2.2	-
18	F	22	1	501-10000	38.8	Yes	14.9	13.6	5.3	4.62	4200	4500	60	229	55	20	67	16	1.52	0.6
19	F	62	4	501-10000	39	Yes	13.5	14.7	4.6	4.38	3700	4300	54	102	16	25	13	24	1.8	1.26
20	M	29	10	501-10000	38.5	Yes	14.5	15.2	5.43	5.53	7000	6000	106	208	21	38	38	40	3.05	0.9
21	F	41	15	501-10000	37.6	Yes	11.9	12.5	4.2	4.24	7900	6100	231	292	52	20	33	18	1	0.65
22	M	19	2	501-10000	37.2	Yes	15.7	15.7	5.4	5.38	5500	6000	120	153	20	28	39	26	1.2	0.7
23	M	20	1	200-300	38	Yes	17	-	5.9	-	7900	-	145	-	26	-	30	-	2	-

24	M	43	5	501-10000	39	Yes	15	14.5	5.46	5.26	10100	6400	168	164	28	25	36	27	1.33	0.69
25	M	37	4	501-10000	37	Yes	15.2	-	4.55	-	6200	-	126	-	22	-	56	-	-	-
26	F	35	4	501-10000	36.8	Yes	14	13.4	4.22	4.5	3000	6000	37	291	16	15	24	20	1.44	1
27	M	19	0	501-10000	40.6	Yes	13.3	14	4.65	4.6	1300	5000	29	220	37	25	30	15	2.03	1.3
28	M	43	1	501-10000	38.8	Yes	13.4	14	4.73	5.4	8000	6990	111	253	31	33	65	60	-	0,4
29	M	34	7	501-10000	36.9	Yes	14	14.1	5	4.96	4700	8000	90	143	70	28	89	40	1.9	1,00
30	M	33	4	301-500	37.5	Yes	15.1	14.5	5.16	5.18	4120	6880	186	353	34	18	12	18	1.3	0,30
31	F	56	1	501-10000	36.1	No	14.3	14.1	5.25	5.16	3000	6280	135	254	30	18	27	18	0.7	0.4
32	M	27	8	501-10000	36	Yes	14.5	13.9	5.66	5.66	5000	6410	85	157	29	22	35	31	1.8	0,4
33	F	23	1	301-500	36.1	Yes	13.1	-	4.6	-	4400	-	119	-	30	-	68	-	1.2	-
34	M	44	10	501-10000	36.2	No	13.2	14.4	4.7	4.81	5000	7670	189	309	24	26	31	37	1	0,9
35	M	24	10	> 10000	36.4	Yes	13.3	-	5	-	8000	-	150	-	44	-	19	-	0.3	-
36	M	28	1	200-300	35.5	Yes	-	16	5.75	-	2300	-	110	51	-	58	-	0.6	-	
37	F	52	0	501-10000	37.5	Yes	13.2	11.3	5.09	4.36	4000	5260	154	284	73	22	48	15	0.3	0,20
38	M	25	0	501-10000	37.3	Yes	15.6	-	5.29	-	2240	-	53	-	107	-	41	-	3.1	-
39	M	36	2	501-10000	39.2	Yes	14.1	-	5.5	-	6790	-	104	-	25	-	35	-	1.5	-
40	M	41	> 20	501-10000	37.3	No	14.2	-	4.95	-	9110	-	170	-	31	-	44	-	1.3	-
41	M	24	> 10	501-10000	36.4	Yes	15.3	-	5.13	-	6400	-	151	-	86	-	260	-	6.5	-
42	F	27	-	501-10000	-	Yes	12.6	-	4.38	-	3700	-	50	-	61	-	130	-	0.97	-
43	F	57	1	501-10000	-	Yes	12.4	-	4.19	-	6460	-	139	-	-	-	-	-	-	-
44	M	33	4	501-10000	36.7	Yes	14.7	-	4.98	-	5400	-	103	-	13	-	26	-	0.7	-
Laboratory reference range values					13.5 - 18		4.5 - 6.5		5000 - 10000		150 - 400		11 - 39		11 - 39		0.4 - 1.2			

^a Not determined

^b AT: Individuals 30-45 days after treatment

Table S3. List of antibodies used in the flow cytometry experiments. Related to Experimental Procedures.

Marker	Fluorochrome	Clone	Company
Anti Human-CD16	PE	B73.1	eBioscience
Anti Human-CD66b	FITC	G10F5	BD
Anti Human-CD15	PercP-Cy5.5	HI98	BD
Anti Human-CD11b	APC	D12	BD
Anti Human-CD117	104D2	0323	eBioscience
Anti Human-CD34	PercP	8G12	BD
Anti Human-CXCR2	PE	48311	R&D systems
Anti Human-CCR5	PE	3A9	BD
Anti Human-CD14	APC	61D3	eBioscience
Anti Human-CD66b	PE	G10F5	BD
Anti Human-HLADR	FITC	LN3	eBioscience
Anti Human-CD8	PercP-Cy5.5	RPA-T8	eBioscience
Anti Human-CD4	APC	RPA-T4	eBioscience
Anti Human-CD3	APC-Cy7	SK7	BD
Anti Mouse-CD45.2	APC-eFluor780	104	eBioscience
Anti Mouse-Ly6G	PE	1A8	BD
Anti Mouse-CD11b	PE-Cy7	M1/70	eBioscience
Anti Mouse-Ly6C	eFluor450	HK1.4	eBioscience
Anti Mouse-CD3	APC-eFluor780	17A2	eBioscience
Anti Mouse-CD4	Pacific Orange	RM4-5	ThermoFisher
Anti Mouse-CD8	Alexa 700	53-6.7	eBioscience

Table S4. Sequences of oligonucleotides used for qRT-PCR reactions. Related to Experimental Procedures.

Oligonucleotides name	Sequence (5' → 3')
GAPDH Fwd	AGGTCGGTGTGAACGGATTG
GAPDH Rev	TGTAGACCATGTAGTTGAGGTCA
CCL3 Fwd	TTCTCTGTACCATGACACTCTGC
CCL3 Rev	CGTCCAATCTTCCGGCTGTAG
CXCL1 Fwd	CTGGGATTCACCTCAAGAACATC
CXCL1 Rev	CAGGGTCAAGGCAAGCCTC
IL-1 β Fwd	ACCTGTCCCTGTGTAATGAAAGACG
IL-1 β Rev	TGGGTATTGCTTGGGATCCA
IFI44 Fwd	TCGATTCCATGAAACCAATCAC
IFI44 Rev	CAAATGCAGAATGCCATGTTT
IRF7 Fwd	CTTCAGCACTTCTTCCGAGA
IRF7 Rev	TGT AGTGTGGTGACCCCTTGC
IFIT1 Fwd	CCTTACAGCAACCATGGGAGA
IFIT1 Rev	GCAGCTTCCATGTGAAGTGAC

SUPPLEMENTAL MOVIE

Movie S1. Related to Figure 5. Neutrophils are recruited to liver sinusoids after *P. chabaudi* infection. Liver intravital microscopy of non-infected and *P. chabaudi*-infected mice. Neutrophils were stained with anti-Ly6G (blue) (clone 1A8) (4 μ g/mouse), and hepatocytes (green) were labeled with sytox green dye (100 μ L/mouse). Time elapsed: 30 minutes.